Crystal Structure of Carboxypeptidase A Complexed with D-Cysteine at 1.75 Å − Inhibitor-Induced Conformational Changes[†,‡]

Daan M. F. van Aalten,[§,||] Curtis R. Chong,[§,⊥] and Leemor Joshua-Tor*

W. M. Keck Structural Biology, Cold Spring Harbor Laboratory, 1 Bungtown Road, Cold Spring Harbor, New York 11724

Received April 26, 2000

ABSTRACT: D-Cysteine differs from the antiarthritis drug D-penicillamine by only two methyl groups on the β-carbon yet inhibits carboxypeptidase A (CPD) by a distinct mechanism: D-cysteine binds tightly to the active site zinc, while D-penicillamine catalyzes metal removal. To investigate the structural basis for this difference, we solved the crystal structure of carboxypeptidase A complexed with D-cysteine (D-Cys) at 1.75-Å resolution. D-Cys binds the active site zinc with a sulfur ligand and forms additional interactions with surrounding side chains of the enzyme. The structure explains the difference in potency between D-Cys and L-Cys and provides insight into the mechanism of D-penicillamine inhibition. D-Cys binding induces a concerted motion of the side chains around the zinc ion, similar to that found in other carboxypeptidase−inhibitor crystal structures and along a limited path. Analysis of concerted motions of CPD and CPD−inhibitor crystal structures reveals a clustering of these structures into distinct groups. Using the restricted conformational flexibility of a drug target in this type of analysis could greatly enhance efficiency in drug design.

Bovine pancreatic carboxypeptidase A (CPD)[1] is one of the best characterized zinc proteases known. It is a digestive enzyme that hydrolyzes C-terminal amino acids from polypeptide substrates (*1*) and serves as a paradigm for understanding zinc protease activity. Several other carboxypeptidases have been identified and are thought to be involved in diverse biological processes. These include the coagulation cascade for carboxypeptidase U (*2*), control of vasoactive peptide levels by lysine carboxypeptidase (*3*), and hormone processing as in the case of carboxypeptidase M (*4*) and E/H. The *fat* mutation in mice, for example, has been mapped to carboxypeptidase E/H (*5*). Carboxypeptidases as well as another family of zinc proteases, namely, the matrix metalloproteases (MMPs), have also been implicated in cancer and inflammation (*3*, *6*, *7*). CPD is a 307-residue exopeptidase, contains one atom of zinc bound at its active site, and is specific for cleavage of large hydrophobic groups at the C-terminus of a protein substrate. The zinc atom is liganded by three residues, namely, His69 (Nδ1), Glu72 (Oϵ1 and Oϵ2), His196 (Nδ1), and a water molecule arranged in a distorted tetrahedral coordination (*8*).

Numerous X-ray crystallographic studies have been conducted on complexes of zinc proteases with zinc-binding inhibitors, many of which are of CPD (ref *9* and references therein and refs *10*−*14*). These studies have focused on a class of inhibitors that bind tightly to the protease in a stable ternary complex between the inhibitor, the enzyme, and the active site zinc, where at least one moiety of the inhibitor ligands the zinc atom. Application of this paradigm to drug development has produced several drugs that target zinc proteases involved in the pathogenesis of diseases such as arthritis, cancer, and hypertension (*15*, *16*). Moreover, structural work contributes to our understanding of the biochemical mechanisms governing zinc protease catalysis.

Compounds containing thiols R-SH are known to inhibit zinc enzymes, notably, MMPs (*17*) and CPDs (*18*), by direct ligation of the sulfhydryl group to the metal. It appears, also, that the strong sulfhydryl−zinc interaction dominates in determining the mode of binding over other factors such as hydrogen bonding to catalytic residues, which are nonetheless important as well (*17*). In fact, sulfhydryl group coordination to zinc is used in procollagenases and progelatinases to keep them in their inactivate, zymogen form. In these cases, their propeptides contain a single cysteine residue that binds via its thiol group to the active site zinc, which remains inactive until the cysteine is removed by proteolysis of the zymogen (*19*). The cysteine ligand is replaced by a water molecule to yield an active enzyme (*20*).

D-Cysteine (D-Cys) and D-penicillamine (D-PEN) (β-β-dimethylcysteine), shown in Figure 1, are sulfhydryl-containing amino acids that differ by only two methyl groups on the β-carbon yet inhibit CPD by distinct mechanisms. D-Cys

[†] This research was supported by an EMBO fellowship (to D.v.A.), grants from the National Science Foundation Research Experiences for Undergraduates Program (DBI-9605102) (to C.R.C), and the Arnold and Mabel Beckman Foundation (to L.J.).

[‡] PDB ID code: 1F57.

* To whom correspondence should be addressed at W. M. Keck Structural Biology, Cold Spring Harbor Laboratory, 1 Bungtown Road, Cold Spring Harbor, NY 11724. Telephone: (516) 367-8821. Fax: (516) 367-8873. E-mail: leemor@cshl.org.

[§] Both authors contributed equally to this work.

[||] Present address: Wellcome Trust Biocentre, Department of Biochemistry, University of Dundee, Dundee DD1 5EH, Scotland, U.K.

[⊥] Undergraduate Research Program, Cold Spring Harbor Laboratory. Present address: Medical Scientist Training Program, Johns Hopkins University School of Medicine, Baltimore, MD 21205.

[1] Abbreviations: CPD, carboxypeptidase A; D-Cys, D-cysteine; D-Cys/CPD, structure of CPD complexed with D-Cys; D-PEN, D-penicillamine; EDTA, ethylenediaminetetraacetic acid; L-Cys, L-cysteine; L-PEN, L-penicillamine; MES, 2-(*N*-morpholino)ethanesulfonic acid; MMPs, matrix metalloproteases; WT-CPD, structure of native, uninhibited CPD.

10.1021/bi000952h CCC: $19.00
Published on Web 07/25/2000

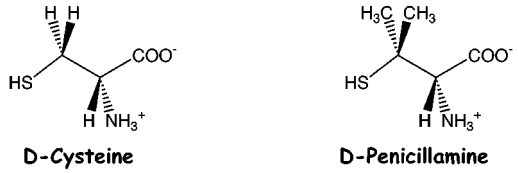

FIGURE 1: Chemical Structure of D-PEN and D-Cys.

binds to the active site zinc in a stable ternary complex. On the other hand, D-PEN removes zinc through an intermediate complex with the enzyme (*21*). The rate for zinc removal by D-PEN is up to 440-fold faster than the spontaneous release (*21*). It appears that the two additional methyl groups on the β-carbon in D-PEN as compared to D-Cys confer a difference in mechanism between the two inhibitors. In addition, D-Cys, with a K_i of 2.3 ± 1.6 μM, is about 500 times more potent an inhibitor than D-PEN (*21*).

Since D-PEN removes the zinc from CPD rapidly, we solved the crystal structure of D-Cys bound to CPD at 1.75-Å resolution and discuss the consequences of adding two methyl groups to its β-carbon. We also discuss the effects of inhibitor stereochemistry on potency. The essential dynamics method is used to correlate the concerted displacements of atoms in the structure to those of CPD−inhibitor complexes deposited in the Protein Data Bank (PDB). We find that the conformational change induced by D-Cys binding can be described in terms of concerted motions of atoms calculated from all other CPD structures. In addition, these eigenvectors allow a classification of CPD conformational states, using only a limited number of variables. Finally, since metal environments within the zinc protease family are similar (*22*), structural interactions between D-Cys and CPD may also be useful in the design of inhibitors for other family members.

MATERIALS AND METHODS

Purification and Crystallization. Bovine carboxypeptidase A (Cox) was purchased from Sigma and used without further purification. Lithium chloride and D-Cysteine (D-Cys) were obtained from Sigma; MES was from Calbiochem. All reagents were reagent-grade or better in terms of purity. Protein concentration was determined based on the absorbance at 280 nm, given an ϵ_{280} for carboxypeptidase A (CPD) of 1.87 mL mg^{-1} cm^{-1} (*23*). CPD was washed three times with water to remove toluene used in packaging and dissolved in 1.2 M LiCl. This stock solution of CPD at 40 mg/mL was then diluted to 15 mg/mL in a solution of 1.2 M LiCl, 25 mM MES, pH 6.0, and 0.5 mM D-Cys. An aliquot of this solution was then pipetted into a 5 μL glass dialysis button. A 6−8 kDa molecular weight cutoff membrane previously washed in water and equilibrated in 0.15 M LiCl was placed over the button and secured with a rubber O-ring. The button was then dialyzed against 0.15 M LiCl, 25 mM MES, pH 6.0, and 0.5 mM D-Cys at 18 °C. Crystals appeared overnight on the bottom and edges of the well.

Data Collection. Diffraction data were collected from a $0.7 \times 0.7 \times 0.1$ mm crystal mounted in a quartz capillary tube at room temperature using a Rigaku-H3R rotating anode source and an RAXIS-II image plate detector. Diffraction data were integrated and scaled with the HKL software package (*24*). See Table 1 for further details.

Table 1: Details of Data Collection[a]

temperature	room temperature
wavelength (Å)	1.54
spacegroup	$P2_1$
cell dimensions (Å)	$a = 44.40$; $b = 57.74$; $c = 58.19$; $\beta = 101.61°$
resolution range (Å)	15.0−1.75 (1.81−1.75)
no. obs reflections	99 346
no. of uniq reflections	28 954 (2679)
redundancy	3.4
$I/\sigma(I)$	14.5 (4.8)
completeness (%)	99.1 (92.9)
R_{merge}	0.065 (0.248)

[a] Values between brackets are for the highest resolution shell.

Table 2: Progress of CPD/D-CYS Refinement in CNS

molecular replacement solution 15.0−3.5 Å	$R = 0.257$; $R_{free} = 0.282$
model building, zinc ion 15.0−2.0 Å	$R = 0.232$; $R_{free} = 0.271$
model building, water molecules 15.0−1.75 Å	$R = 0.152$; $R_{free} = 0.185$
inhibitor, water molecules 15.0−1.75 Å	$R = 0.144$; $R_{free} = 0.178$
model building, alternate conformations 15.0−1.75 Å	$R = 0.143$; $R_{free} = 0.176$
final model (0.0 σ cutoff) 15.0−1.75 Å	$R = 0.138$; $R_{free} = 0.165$
final model (2.0 σ cutoff) 15.0−1.75 Å	$R = 0.133$; $R_{free} = 0.159$
no. of atoms	2437 protein; 261 water; 1 Zn; 7 D-Cys
no. of side chain alternate conformations	11
rmsd bonds (Å)	0.011
rmsd angles (°)	1.46
protein average B-factor (Å^2)	14.9

Solution and Refinement. The D-Cys/CPD structure, with one model in the asymmetric unit, was solved by molecular replacement using AMoRe (*25*) with a CPD structure from PDB entry 5CPA (*8*) excluding the zinc as a search model. Using 8.0−4.0 Å data, the sequential rotational and translational searches gave a single solution with an *R*-factor of 0.276 and a correlation coefficient of 0.791, after rigid body refinement in AMoRe. Further refinement was performed with CNS (*26*) with iterative model building in O (*27*). In the initial F_o-F_c map, a strong peak between the metal binding residues indicated the location of the zinc ion, which was included in subsequent refinement. Progress of the refinement is detailed in Table 2. After a few cycles of model building and placement of some well-defined water molecules (4σ peaks in a F_o-F_c map and at least one hydrogen bond to the protein), the D-Cys inhibitor could be clearly seen in the F_o-F_c maps (Figure 2) and was built into the model. Further rounds of model building and refinement allowed placement of additional water molecules and assignment of some alternate side chain conformations (Table 2).

Analysis of the Conformational Change Induced by Inhibitor Binding. The structural differences between the uncomplexed CPD structure (WT-CPD) and the structure presented here of CPD with D-cysteine (D-Cys/CPD) were analyzed in terms of concerted displacements of atoms using the essential dynamics method (*28*). With this method, it is possible to describe protein conformational freedom using a small number of variables, calculated from an ensemble of structures (e.g., refs *29* and *30*). Traditionally, such ensembles of structures have been obtained from computer

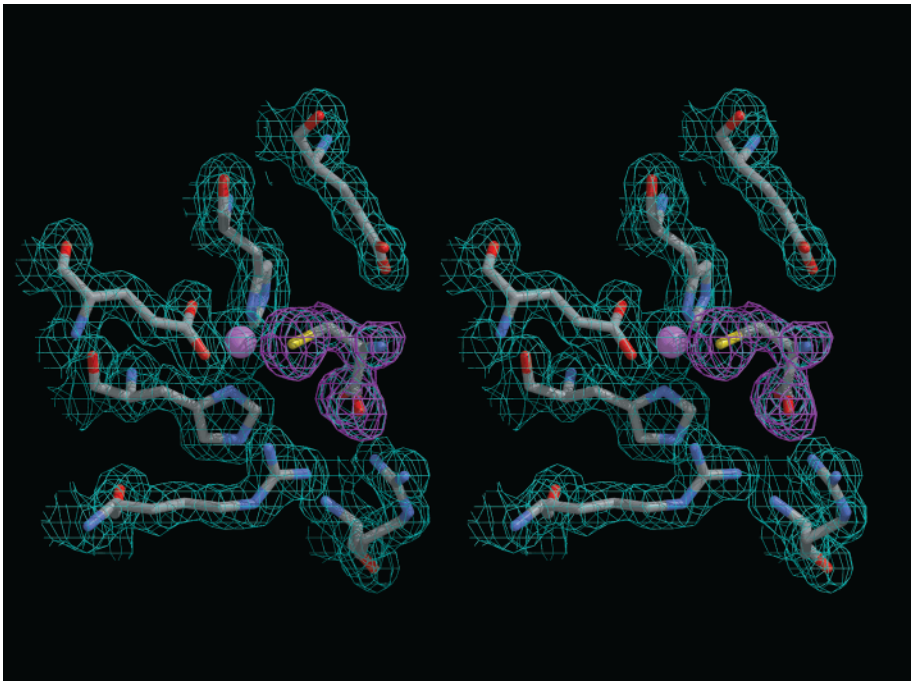

FIGURE 2: Electron density around the D-cysteine inhibitor. The F_o-F_c map just before including the inhibitor is shown in magenta. The $2F_o-F_c$ map after building in the inhibitor and subsequent refinement is shown in cyan. σ levels were 1.0 and 2.5 for the $2F_o-F_c$ and F_o-F_c maps, respectively. Zinc ion is shown as a pink sphere. This figure as well as Figures 3A, 4, 5, and 7 were prepared using Molscript (*63*), Bobscript (*64*) and Raster 3D (*65*, *66*).

simulations (*31*−*33*). Recently, however, it has been shown that groups of related crystal structures can also yield an ensemble from which large concerted motions can be calculated with essential dynamics (*34*, *35*). The essential dynamics method is based on diagonalization of the atomic covariance matrix, yielding a set of eigenvectors and eigenvalues. The eigenvectors describe concerted displacements of certain groups of atoms, and the eigenvalues are the amplitudes of these motions. Such descriptions of concerted motions have proved useful in linking dynamic properties of proteins to their functions in a number of cases (*29*−*31*, *36*−*38*).

Here, we used an ensemble of all zinc-containing CPD crystal structures available in the PDB database of protein structures (*39*), prepared according to a procedure described before (*33*). In addition to wild-type CPD (PDB entries: 5CPA (*8*), 1YME, and 2CTB), the following PDB entries describing CPD complexes with various inhibitors were used: 1BAV, 1CBX (*40*), 1CPS (*12*), 2CTC, 3CPA (*41*), 4CPA (*42*), 6CPA (*43*), 7CPA (*11*) and 8CPA (*11*). Crystal structures with more than one molecule per asymmetric unit were treated separately. All these structures were superimposed onto the coordinates from 5CPA to remove translational and rotational motion. A set of atoms was selected, consisting of the zinc and both primary and secondary protein side chain ligands. A covariance matrix was built from this subset of atomic coordinates and diagonalized. The resulting eigenvectors describe concerted conformational changes of residues in the active site. Conformational changes were then studied by projecting the crystal structures onto the eigenvectors.

RESULTS

D-Cysteine Interaction with CPD. The crystal structure of the complex of D-cysteine with CPD was solved to 1.75-Å resolution. These crystals belong to a different crystal form than previously described crystals of CPD with or without inhibitors. The structure was solved by molecular replacement using the free enzyme and excluding the zinc atom. The electron density maps (Figure 2) show D-cysteine buried in the active site of the protein and bound to the catalytic zinc via its sulfur. This is the first crystal structure of a thiol inhibitor bound to CPD. The thiolate of D-Cys has replaced the active site water and coordinates zinc in a distorted tetrahedral geometry, similar to that observed in the crystal structure of (2-benzyl-3-mercaptopropanoyl)-L-alanylglycinamide, a mercaptan inhibitor, bound to thermolysin, another zinc protease (*44*). The $Zn^{2+}-S$ bond distance is 2.2 Å, corresponding to the average distance of 2.1 Å between Zn(II) and cysteine for 14 independent structures in the PDB, and the $C\beta-S-Zn^{2+}$ angle is 109°, also similar to the average torsion angle of 112° observed in this PDB survey (*45*). This is consistent with previous spectroscopic studies that show that the thiolate of D-Cys binds to the active site metal of a cobalt-substituted CPD (*21*).

In addition to the zinc−sulfur bond, D-Cys is tethered to the active site by additional contacts, electrostatic and hydrogen bonded, to protein residues (Figure 3, Table 3). The positively charged amino group of D-Cys interacts with the negatively charged carboxylate of Glu270 ($N_{D-Cys}-O\epsilon1_{E270}$ 2.85 Å). The D-Cys carboxylate also forms salt bridges with the guanidinium groups of Arg127 and Arg145 and hydrogen bonds to Asn144. All of these residues are thought to be important in catalysis. Glu270 acts as a general base, abstracting a proton from the zinc-bound water to form a hydroxyl anion nucleophile (*46*, *47*). Asn144 and Arg145 bind the C-terminal substrate carboxylate, and Arg127 stabilizes the oxyanion generated during the transition state. Upon D-Cys binding, the side chains of three of these residues, Arg127, Arg145, and Glu270 move toward the

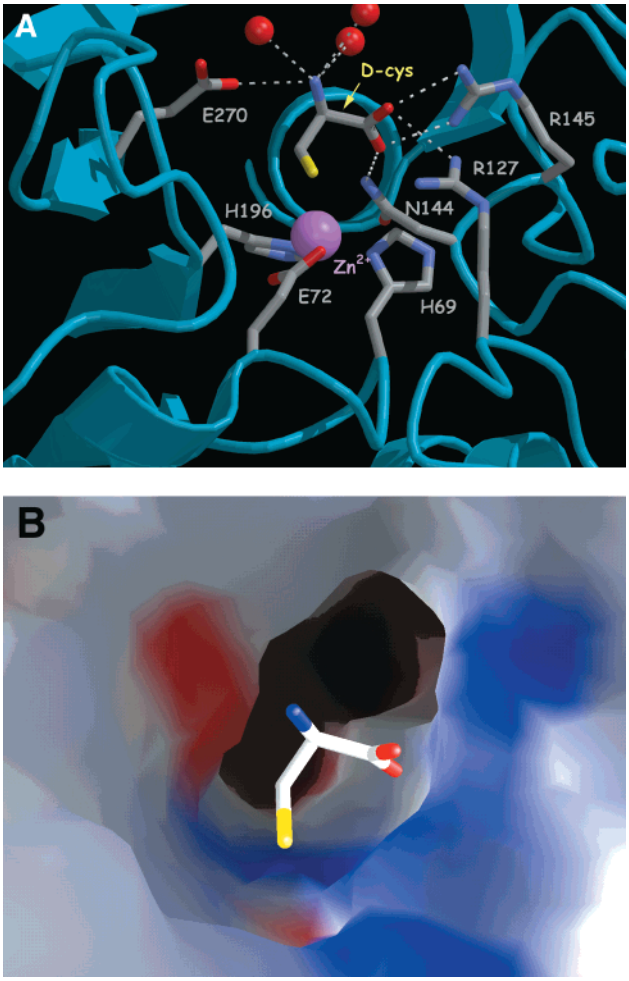

FIGURE 3: (A) Details of interaction between the protein active site residues and the inhibitor. The protein backbone is shown in ribbons representation (cyan). Active site residues and zinc ligands are shown using sticks, colored by atom type, water molecules are represented by red spheres. Hydrogen bonds between the inhibitor and protein/water are shown by dotted white lines. (B) Electrostatic surface potential in the active site. GRASP (*67*) electrostatics calculations were performed using the appropriate full charges assigned to Asp, Gly, Lys, and Arg and a charge of +2.0 on the zinc ion. A molecular surface was calculated and colored by electrostatic potential from red (<20.0 k_BT) to blue (>20.0 k_BT). The inhibitor structure is shown in a stick representation.

Table 3: Distances of D-Cys/CPD Interactions

enzyme or water atom	D-Cys atom	distance (Å)[a]
zinc	Sγ	2.2
Glu270 Oϵ1	amino N	2.9*
Asn144 Nδ2	carboxylate O1	3.0*
Arg145 Nη1	carboxylate O1	2.8*
Arg145 Nη1	carboxylate O2	3.5
Arg145 Nη2	carboxylate O2	3.1*
Arg127 Nη2	carboxylate O2	3.1*
O_{water} 502	amino N	3.3*
O_{water} 740	amino N	3.2*
O_{water} 761	amino N	3.0*
O_{water} 761	carboxylate O2	3.5

[a] Atoms that form a hydrogen bond as judged by distance and geometric criteria are denoted by an asterisk (*).

charged groups of the inhibitor. The D-Cys inhibitor as well as the active site residues interacting with the inhibitor are well-ordered with an average B-factor of 17.6 Å^2 for the inhibitor atoms and 11.5 Å^2 for the active site residues. In addition, D-Cys is engaged in hydrogen bonding interactions with three water molecules (W502, W740, and W761) via its amino group (Figure 3A). Similar interactions with active site residues Glu270, Arg127, and Arg145 have been previously reported for other CPD inhibitors (reviewed in ref *48*)

No significant changes are observed for protein ligands to the zinc upon D-Cys binding. In several CPD−inhibitor complexes, the active site zinc is observed to move in the direction of Arg127. This change is attributed to the flexibility of the interaction between the zinc and the protein ligand Glu72 (*9*, *12*) since motion of the active site zinc toward Arg127 is coordinated with a change in Glu72 binding from a bidentate to a monodentate metal ligation. However, in the D-Cys/CPD complex, Glu72 remains a bidentate ligand, and the zinc atom does not move. The active site zinc and its protein ligands are also well-ordered and have low B-factors of 10.8 and 7.6 Å^2 in average, respectively.

Tyr248 is thought to play an important role in substrate binding during CPD catalysis (*49*). In structures of CPD bound to transition-state analogue inhibitors, Tyr248 is observed to swivel by 12 Å to donate a hydrogen bond to the inhibitor carboxylate. The scale of this movement was presented as evidence in support of the "induced fit" hypothesis of enzyme action (*50*, *51*). However, there is an orthorhombic crystal form of native CPD in which Tyr248 is positioned inside the active site similar to its conformation when a substrate is bound (*52*). Although Tyr248 swivels 8.4 Å around the Cα−Cβ bond in the D-Cys/CPD complex structure as compared to native CPD, this rotation does not bring it into the active site in position to interact with the D-Cys carboxylate. Rather, this rotation brings the tyrosine side chain to a position about halfway between the two conformations, approximately perpendicular to both. In the native monoclinic structure, this tyrosine is involved in crystal packing contacts, mostly through nonpolar contacts but also hydrogen bonding through a water molecule to a symmetry-related molecule. In the D-Cys/CPD structure, the packing environment is different; however, Tyr248 is also involved in crystal contacts through water molecules. The absence of the interaction with the inhibitor in this case may be a factor in the higher K_i of D-Cys as compared to CPD inhibitors that hydrogen bond to Tyr248. Indeed, mutation of Tyr248 to phenylalanine increases the K_i of potato carboxypeptidase inhibitor by 70-fold without affecting the catalytic constant, k_{cat}, toward peptide substrates (*53*).

Beyond the active site, there is little difference in the D-Cys/CPD complex structure as compared to native CPD, with a root-mean-square (RMS) deviation between this complex and 5CPA (*8*) of 0.35 Å for Cα atoms. Even though our crystals were grown overnight in a 0.5 mM D-Cys solution, the disulfide bond between Cys138 and Cys161 remains intact, and no reduction is observed. This crystal structure represents a new crystal form for CPD. The absence of conformational changes outside the active site suggests that aside from Tyr248 discussed above, the crystal packing forces for this new crystal form do not affect secondary and tertiary structure.

D-Cysteine-Induced Concerted Conformational Changes. Previous studies of concerted motions on the basis of molecular dynamics computer simulations (*29*, *30*, *36*), NMR ensembles (*38*, *54*, *55*), and crystal structures (*34*, *35*) have shown that such motions may play a role in protein function.

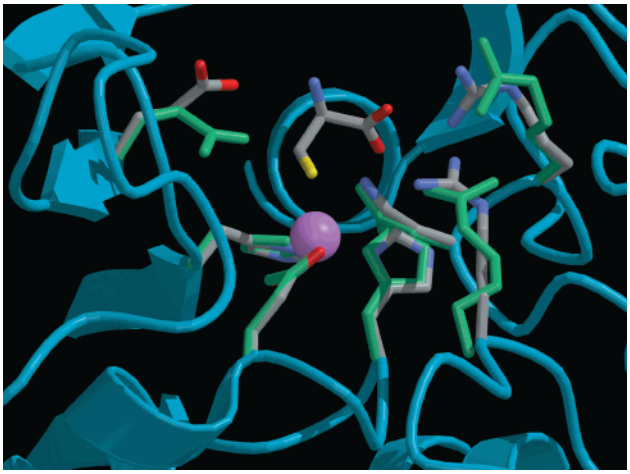

FIGURE 4: Conformational changes in the active site. WT-CPD and D-Cys/CPD structures were superimposed using their α-carbons shown in the same orientation as in Figure 3A. The D-Cys/CPD backbone is shown in ribbon representation (cyan). Primary and secondary zinc ligands are shown for D-Cys/CPD (colored by atom type) and WT-CPD (green).

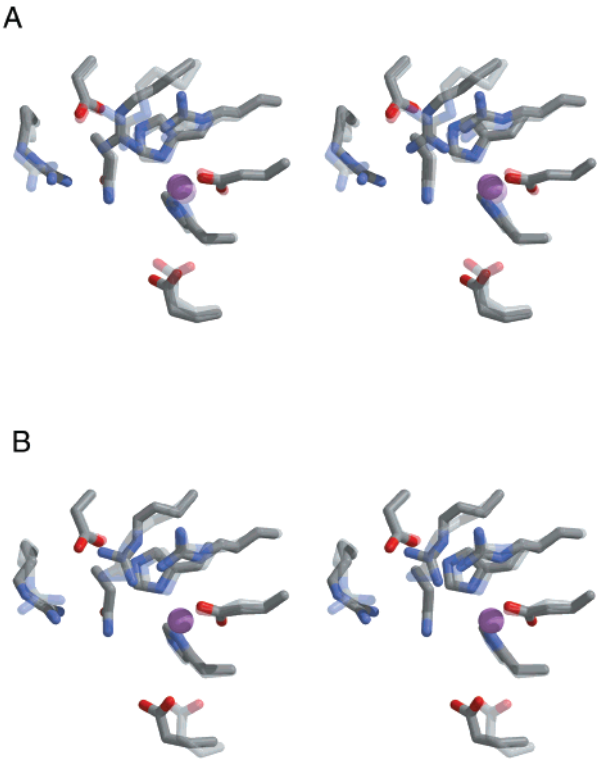

FIGURE 5: Motion along eigenvector 1 (A) and eigenvector 2 (B) calculated from the ensemble of crystal structures. For each eigenvector, two structures are superimposed: the structure with the lowest projection (least transparent) and the highest projection (most transparent).

In CPD, one might expect to observe concerted motions of active site residues involved in substrate binding and catalysis. Here, we attempt to describe all active site conformations possible using a few variables, rather than large sets of Cartesian coordinates, by analysis of crystal structures using the "essential dynamics" technique. A straightforward comparison of WT-CPD and D-Cys/CPD structures reveals that several active site residues change conformation (Figure 4). As mentioned above, Arg127, Arg145, and Glu270 move toward the charged groups on the D-Cys inhibitor. It is

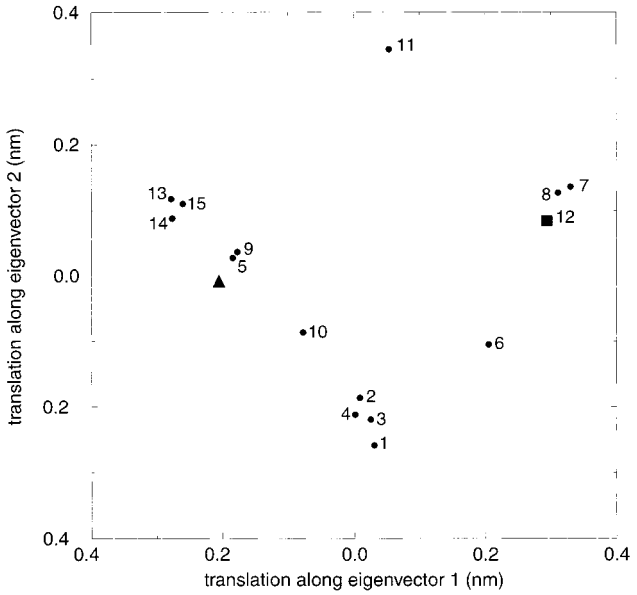

FIGURE 6: Projection of CPD crystal structures on the first two eigenvectors. Structures of D-Cys/CPD (triangle), WT-CPD (square), and the those mentioned in Materials and Methods (circles) were projected on eigenvector 1 and 2 calculated from the ensemble of crystal structures and labeled. Inner products resulting from this projection indicate how much the conformation has changed along these eigenvectors starting from the average crystal structure and are then combined in this two-dimensional scatter plot. Labels are as follows: (1) 1BAV (complex with 2-benzyl-3-iodo-propionate) − molecule 1; (2) 1BAV − molecule 2; (3) 1BAV − molecule 3; (4) 1BAV − molecule 4; (5) 1CBX (complex with L-benzylsuccinate); (6) 1CPS (complex with a sulfodiimine); (7) 1YME (native with mercury); (8) 2CTB (native); (9) 1CTB (complex with L-phenyl lactate); (10) 3CPA (complex with glycyl-L-tyrosine); (11) 4CPA (complex with potato inhibitor); (12) 5CPA (native); (13) 6CPA (complex with Bz-Ala-Ala-PO-Phe); (14) 7CPA (complex with Bz-Phe-Val-PO-Phe); (15) 8CPA (complex with Bz-Ala-Gly-PO-Phe).

interesting to see how this movement compares to that observed in other CPD structures. Using the procedure outlined in Materials and Methods, the zinc as well as primary and secondary zinc ligand residues were extracted from CPD crystal structures in the PDB, a covariance matrix was built, and eigenvectors/values were calculated by diagonalization. Each eigenvector describes an independent motion consisting of concerted displacements of atoms. The motions along eigenvectors 1 and 2 (those with the two largest eigenvalues) show that the motions of residues in the active site are highly correlated (Figure 5). Especially Arg127, Arg145, and Glu270 show large motions similar to those in Figure 4. In fact, if a normalized vector is drawn in configurational space between the WT-CPD and the D-Cys/CPD structures, this vector has an inner product of 0.625 with the first eigenvector calculated from the crystal structures. Note that these structures include WT-CPD but not the D-Cys/CPD structure described here. This indicates that the conformational change necessary to move from WT-CPD to D-Cys/CPD is already described by the crystal structures in the database. Thus, this conformational change can, for a large part, be captured by a single variable rather than by lists of Cartesian coordinates, namely, the translation along eigenvector 1. This description allows study and classification carboxypeptidase structures by their position along the first or the first few eigenvectors. The projections along eigenvector 1 and eigenvector 2 are shown in Figure 6. It is worth

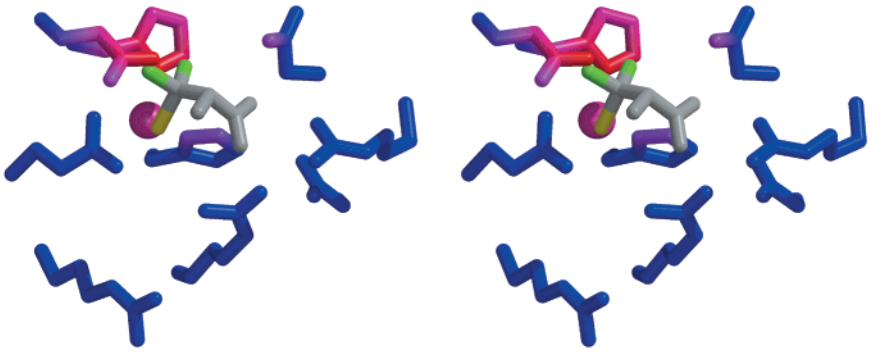

FIGURE 7: Steric clashes introduced by inclusion of two extra methyl groups on the α-carbon of D-Cys. Atoms in the active site are colored from blue (>5 Å distance to either of the extra methyl groups) to red (2.1 Å distance to either of the extra methyl groups). D-Cys is shown in gray, except for the methyl groups (green) and sulfur (yellow).

noting that the crystal structures are spread out along the individual eigenvectors, indicating that these eigenvectors are not simply describing the transition from one conformational state to another. However, it is possible to classify CPD structures according to their translations along these eigenvectors. For instance, the three native CPD structures seem to cluster around a similar position along both eigenvector 1 and eigenvector 2 (around the WT, 5CPA position). The structures of transition-state analogue inhibitors the phosphonate, ZAF [Bz-Ala-Ala^{P}(O)-Phe], FVF [Bz-Phe-Val^{P}(O)-Phe], and AGF [Bz-Ala-Gly^{P}(O)-Phe] (6CPA, 7CPA, and 8CPA, respectively) (*11*, *43*) and inhibitors mimicking the products of peptide hydrolysis L-benzylsuccinate and L-phenyllactate (1CBX and 2CTC, respectively) (*40*) are scattered around the CPD/D-Cys structure reported here (Figure 6). Between these latter structures and native CPD structures lie complexes of CPD with BIP (2-benzyl-3-iodopropanoic acid) (*56*), glycyl-L-tyrosine (*41*), and the potato inhibitor (*42*) (1BAV, 3CPA, and 4CPA, respectively), which do not mimic intermediates along the carboxypeptidase substrate hydrolysis reaction. The amount of concerted motion along eigenvector 1 describing the translation from the wild-type CPD structure to the transition state analogue and product inhibitors is similar to that observed from CPD to D-Cys/CPD. This suggests that binding of D-Cys to CPD induces a conformational change in active site residues similar to that observed for transition-state analogue and product inhibitors. Thus, structures with similar properties have more or less similar translations along the eigenvectors, yet the spread is large enough to permit calculation of the eigenvectors.

Possible Implications for CPA Interaction with D-PEN. As mentioned earlier, D-PEN inhibits CPD by catalyzing zinc dissociation from the enzyme active site (*21*). This occurs with crystalline CPD as well, thus complicating crystallographic studies of an intermediate in this reaction. To gain insight into the mechanism of inhibition for D-PEN and the reasons underlying the differences with the mechanism of D-Cys, we used the D-Cys/CPD complex structure to study the putative effects of adding two methyl groups to the D-Cys β-carbon. Using standard tetrahedral geometry, two methyl groups were added to D-Cys to generate a D-PEN structure, which was energy-minimized using PRODRG (*57*) and GROMOS87 (*58*) and superimposed onto D-Cys in the D-Cys/CPD complex structure. For this analysis, we considered distances of < 3.5 Å between nonbonded atoms, which cannot hydrogen bond, as steric clashes. If D-PEN were to bind to CPD in the same orientation as D-Cys, the two added methyl groups would clash with His196, Glu270, and the zinc ion (Figure 7). Thus, it seems that D-PEN would significantly perturb active site residues if it bound in this orientation. On the other hand, if D-PEN were to bind in a different orientation, favorable interactions between the charged groups on D-PEN with Arg127, Arg145, Asn144, and Glu270 would probably be lost (Figure 3).

DISCUSSION

D-Cys is a CPD inhibitor that binds to the active site metal via a thiol ligand. The crystal structure of D-Cys complexed with CPD reveals many other interactions that are involved in binding. D-Cys takes advantage of the electrostatic and hydrogen-bonding interactions in the CPD active site along with a complementary steric fit to effect inhibition. To accommodate D-Cys binding, four active site residues change conformation to optimize electrostatic interactions (Figure 4). In effect, the active site residues become secondary ligands to the zinc through their interactions with D-Cys. Their contribution to the avidity of D-Cys binding is analogous to the effect of secondary ligands in orienting protein side chains for optimal ligation to the metal. Several inhibitors take advantage of the specificity of CPD for aromatic or branched aliphatic side chains C-terminal to the scissile bond position (the S1′ position) of a substrate (*47*, *49*). Although D-Cys lacks an aromatic or aliphatic side chain at P1′ and does not bind to the S1′ pocket, it has a relatively high affinity for CPD, with a K_i 20-fold lower than D-Phe, for example (*59*). The interactions between the carboxylate and amino groups of D-Cys and D-Phe and the active site Glu270 and Arg145 are similar (*49*), although the D-Cys carboxylate forms additional hydrogen bonds with Arg-127 and Asn-144. It appears that the metal-binding properties of the thiol group together with the hydrogen bonding network in the active site compensate for lack of favorable interactions between D-Cys and the S1′ pocket of the enzyme.

As mentioned, several active site residues move upon inhibitor binding. Our analysis of concerted motions in the CPD active site for this structure and other CPD inhibitors found in the PDB, shows that the residues participating in substrate binding and catalysis move through strongly correlated motions. We show that active site conformational substates could be captured using only one or two parameters, which can be used for classification of inhibitors. Starting from the native CPD structures, different inhibitors induce

conformational change to a different extent but always along a path enforced by the protein structure and captured in our essential dynamics eigenvectors. Three clusters of structures were identified by similar eigenvector projections (Figure 6): native CPD, CPD complexed to transition state or product analogues, and "others". While the latter are chemically unrelated, they are distinct from the other two groups. The potato inhibitor (4CPA) is a protein that binds to the active site zinc through a C-terminal carboxylate, as well as through extensive protein−protein interactions; 2-benzyl-3-iodopropionate (1BAV) is an irreversible inhibitor that forms a covalent ester linkage with Glu270 (*56*); the peptide glycyl-L-tyrosine (3CPA) is a slowly hydrolyzed substrate. Interestingly, the active site conformation of D-Cys/CPD appears to fall near the cluster of transition state analogues. It appears, therefore, that D-Cys induces a conformational state of the active site similar to that observed for transition state analogues (Figure 6). Using the limited conformational flexibility of a drug target, as shown here with CPD, could greatly assist in enhanced drug design capabilities, by allowing such flexibility, without an enormous penalty in computation time.

The greater potency of zinc-binding ligands with D stereochemistry has been noted for inhibitors of many zinc enzymes including carboxypeptidase, angiotensin converting enzyme, and thermolysin (*15*). In these inhibitor families, the lower potency of L-enantiomers is attributed to suboptimal interaction with the enzyme active site. The D-Cys/CPD structure reported here extends this observation to L-Cys. If L-Cys binds zinc with its thiol as D-Cys does, at least one of the favorable interactions with an active site residue is lost. Specifically, the L-enantiomer cannot form electrostatic and hydrogen bond interactions with both Glu270 and the asparagine and two arginine residues at the same time. This loss raises the L-Cys K_i by 150-fold as compared to D-Cys (*21*) and indicates the importance of such an interaction in determining inhibitor potency.

Although the cysteine compounds tested are weaker inhibitors of thermolysin (TLN) than CPD, there is a similar difference in enantiomer potency. L-Cys is 42-fold less potent an inhibitor for TLN than D-Cys, as compared to an 87-fold difference for CPD (*21*). This is consistent with the similarity in active site geometry between TLN and CPD. In TLN, the position of Glu143, which acts as a general base in catalysis, overlaps its CPD counterpart, Glu270 (*60*). The positively charged arginine cluster in CPD is replaced by His231, which is also thought to stabilize the oxyanion transition state (*61*). Consequentially, the 10-fold lower potency of D-Cys toward TLN as compared to CPD may be due to replacement of the positively charged arginine residues with a neutral histidine residue, which can only form a single hydrogen bond rather than the two that the guanidinium group can form.

In contrast, the differences between D- and L-Cys inhibitor potency is only 2-fold for matrilysin (MAT), a matrix metalloprotease [$K_i = 0.75$ and 1.6 mM, respectively (*21*)]. An overlap of the MAT and CPD active site shows that there are no residues in MAT equivalent to Arg127 and Arg145, which stabilize the D-Cys carboxylate in CPD (Figures 3 and 4). In addition, the active site Glu198 in MAT is surrounded by hydrophobic residues that are thought to increase its pK_a [Chong and Auld, unpublished data; (*62*)] which, in turn, may result in decreased binding to the amino group of the inhibitor.

D-PEN has been used to treat rheumatoid arthritis for the past 35 years. Rapid-scanning stopped-flow spectroscopy indicates D-PEN binds to Co−CPD differently than D-Cys (*21*). No cobalt−sulfur bond is formed in the intermediate that is formed within the mixing time of the instrument. Cobalt is then released from the enzyme with a half-life of 0.5 s. The results of model building D-PEN complexes of CPD are consistent with these results. If D-PEN bound to CPD in the same orientation as D-Cys, it is apparent from model building that D-PEN would disrupt active site residues crucial for effective chelation of zinc by the enzyme and thus reduces the inherent affinity of the protein for zinc (Figure 7). The putative steric clash between the D-PEN methyl groups and the zinc ligand His196, the secondary ligand Glu270 and zinc itself would disrupt the coordination sphere resulting in zinc dissociation. To minimize the steric clash between Glu270 and the D-PEN methyl groups, the active site zinc may move toward Arg127 and change Glu72 ligation to monodentate. This motion and the change in Glu72 binding are observed in other CPD−inhibitor structures and could reduce protein metal affinity (*9*). Steric hindrance of the extra methyl groups may force D-PEN to bind zinc in the active site in a somewhat different orientation, and the lack of favorable contacts observed for D-Cys could cause D-PEN to dissociate with the zinc. Thus even though two zinc-binding inhibitors may be similar in chemical structure, basic substituency can have pronounced and unexpected effects on mechanism and potency.

ACKNOWLEDGMENT

We are grateful to Dr. David Auld for comments and advice and thank him and Dr. Douglas Rees for critical reading of the manuscript. We also thank the members of the L.J. group for fruitful discussions.

REFERENCES

1. Vallee, B. L., Galdes, A., Auld, D. S., and Riordan, J. F. (1983) in *Zinc Enzymes* (Spiro, T. G., Ed.) pp 26−75, John Wiley, New York.
2. Hendriks, D. F. (1998) in *Handbook of Proteolytic Enzymes* (Barrett, A. J., Rawlings, N. D., and Woessner, J. F., Eds.) pp 1328−1330, Academic Press, London.
3. Skidgel, R. A., and Erdös, E. G. (1998) in *Handbook of Proteolytic Enzymes* (Barrett, A. J., Rawlings, N. D., and Woessner, J. F., Eds.) pp 1344−1347, Academic Press, London.
4. Skidgel, R. A. (1998) in *Handbook of Proteolytic Enzymes* (Barrett, A. J., Rawlings, N. D., and Woessner, J. F., Eds.) pp 1347−1349, Academic Press, London.
5. Fricker, L. D. (1998) in *Handbook of Proteolytic Enzymes* (Barrett, A. J., Rawlings, N. D., and Woessner, J. F., Eds.) pp 1341−1344, Academic Press, London.
6. Lochter, A., Sternlicht, M. D., Werb, Z., and Bissell, M. J. (1998) *Ann. N.Y. Acad. Sci. 857*, 180−193.
7. Coussens, L. M., and Werb, Z. (1996) *Chem. Biol. 3*, 895−904.
8. Rees, D. C., Lewis, M., and Lipscomb, W. N. (1983) *J. Mol. Biol. 168*, 367−387.
9. Christianson, D. W., and Lipscomb, W. N. (1989) *Acc. Chem. Res. 22*, 62−69.
10. Kaplan, A. P., and Bartlett, P. A. (1991) *Biochemistry 30*, 8165−8170.
11. Kim, H., and Lipscomb, W. N. (1991) *Biochemistry 30*, 8171−8180.
12. Cappalonga, A. M., Alexander, R. S., and Christianson, D. W. (1992) *J. Biol. Chem. 267*, 19192−19197.
13. Gomez-Ortiz, M., Gomis-Ruth, F. X., Huber, R., and Aviles, F. X. (1997) *FEBS Lett. 400*, 336−340.

14. Chai, J. J., He, C., Li, M., Tang, L., and Luo, M. (1998) *Protein Eng. 11*, 841−845.
15. Ondetti, M. A., Rubin, B., and Cushman, D. W. (1977) *Science 196*, 441−444.
16. Blundell, T. L. (1994) *Nat. Struct. Biol. 1*, 73−75.
17. Schwartz, M. A., Venkataraman, S., Ghaffari, M. A., Libby, A., Mookhtiar, K. A., Mallya, S. K., Birkedal-Hansen, H., and van Wart, H. E. (1991) *Biochem. Biophys. Res. Commun. 176*, 173−179.
18. Holmquist, B., and Vallee, B. L. (1979) *Proc. Natl. Acad. Sci., U.S.A. 76*, 6216−6220.
19. Springman, E. B., Angleton, E. L., Birkedal-Hansen, H., and van Wart, H. E. (1990) *Proc. Natl. Acad. Sci., U.S.A. 87*, 364−368.
20. Vallee, B. L., and Auld, D. S. (1990) *Biochemistry 29*, 5647−5659.
21. Chong, C. R., and Auld, D. S. (2000) *Biochemistry 39*, 7580−7588.
22. Feinberg, H., Greenblatt, H. M., Behar, V., Gilon, C., Cohen, S., Bino, A., and Shoham, G. (1995) *Acta Crystallogr. D51*, 428−429.
23. Simpson, R. T., Riordan, J. F., and Vallee, B. L. (1963) *Biochemistry 2*, 616−622.
24. Otwinowski, Z., and Minor, W. (1997) *Methods Enzymol. 276*, 307−326.
25. Navaza, J., and Saludjiam, P. (1994) *Acta Crystallogr. A50*, 157−163.
26. Brünger, A. T., Adams, P. D., Clore, G. M., Gros, P., Grosse-Kunstleve, R. W., Jiang, J.-S., Kuszewski, J., Nilges, M., Pannu, N. S., Read, R. J., Rice, L. M., Simonson, T., and Warren, G. L. (1998) *Acta Crystallogr. D54*, 905−921.
27. Jones, T. A., Zou, J. Y., Cowan, S. W., and Kjeldgaard, M. (1991) *Acta Crystallogr. A47*, 110−119.
28. Amadei, A., Linssen, A. B. M., and Berendsen, H. J. C. (1993) *Proteins 17*, 412−425.
29. van Aalten, D. M. F., Findlay, J. B. C., Amadei, A., and Berendsen, H. J. C. (1995) *Prot. Eng. 8*, 1129−1135.
30. Mello, L. V., van Aalten, D. M. F., and Findlay, J. B. C. (1998) *Biochemistry 37*, 3137−3142.
31. van Aalten, D. M. F., Amadei, A., Bywater, B., Findlay, J. B. C., Berendsen, H. J. C., Sander, C., and Stouten, P. F. W. (1996) *Biophys. J. 70*, 684−692.
32. Peters, G. H., van Aalten, D. M. F., Edholm, O., Toxvaerd, S., and Bywater, R. (1996) *Biophys. J. 71*, 2245−2255.
33. de Groot, B. L., Amadei, A., van Aalten, D. M. F., and Berendsen, H. J. C. (1996) *J. Biomol. Struct. Dyn. 13*, 741−751.
34. van Aalten, D. M. F., Conn, D. A., de Groot, B. L., Berendsen, H. J. C., Findlay, J. B. C., and Amadei, A. (1997) *Biophys. J. 73*, 2891−2896.
35. de Groot, B. L., Haywood, S., van Aalten, D. M. F., Amadei, A., and Berendsen, H. J. C. (1998) *Proteins 31*, 116−127.
36. van Aalten, D. M. F., Amadei, A., Linssen, A. B. M., Eijsink, V. G. H., Vriend, G., and Berendsen, H. J. C. (1995) *Proteins 22*, 45−54.
37. Mello, L. V., van Aalten, D. M. F., and Findlay, J. B. C. (1997) *Prot. Eng. 10*, 381−387.
38. van Aalten, D. M. F., Grotewold, E., and Joshua-Tor, L. (1998) *Methods 14*, 318−328.
39. Bernstein, F. C., Koetzle, T. F., Williams, G. J. B., Meyer, E. F., Brice, M. D., Rodgers, J. R., Kennard, O., Shimanouchi, T., and Tasumi, M. (1977) *J. Mol. Biol. 112*, 535−542.
40. Mangani, S., Carloni, P., and Orioli, P. (1992) *J. Mol. Biol. 223*, 573−578.
41. Christianson, D. W., and Lipscomb, W. N. (1986) *Proc. Natl. Acad. Sci., U.S.A. 83*, 7568−7572.
42. Rees, D. C., and Lipscomb, W. N. (1982) *J. Mol. Biol. 160*, 475−498.
43. Kim, H., and Lipscomb, W. N. (1990) *Biochemistry 29*, 5546−5555.
44. Monzingo, A. F., and Matthews, B. W. (1982) *Biochemistry 21*, 3390−3394.
45. Chakrabarti, P. (1989) *Biochemistry 28*, 6081−6085.
46. Auld, D. S. (1987) in *Enzyme Mechanisms* (Page, M., and Williams, A., Eds.) pp 240−258, Royal Society of Chemistry, London.
47. Christianson, D. W., and Lipscomb, W. N. (1988) in *Mechanistic Principles of Enzyme Activity* (Liebman, A. G., Ed.) pp 1−25.
48. Auld, D. S. (1998) in *Handbook of Proteolytic Enzymes* (Barrett, A. J., Rawlings, N. D., and Woessner, J. F., Eds.) pp 1321−1326, Academic Press, London.
49. Christianson, D. W., Mangani, S., Shoham, G., and Lipscomb, W. N. (1989) *J. Biol. Chem. 264*, 12849−12853.
50. Koshland, D. E. (1958) *Proc. Nat. Acad. Sci. U.S.A. 44*, 98−104.
51. Lipscomb, W. N., George, N., Reeke, J., Hartsuck, J. A., Quiocho, F. A., and Bethge, P. H. (1970) *Philos. Trans. R. Soc. London B 257*, 177−214.
52. Bukrinsky, J. T., Bjerrum, M. J., and Kadziola, A. (1998) *Biochemistry 37*, 16555−16564.
53. Gardell, S. J., Craik, C. S., Hilvert, D., Urdea, M. S., and Rutter, W. J. (1985) *Nature 317*, 551−555.
54. de Groot, B. L., van Aalten, D. M. F., Scheek, R. M., Amadei, A., Vriend, G., and Berendsen, H. J. C. (1997) *Proteins 29*, 240−251.
55. Abseher, R., Horstink, L., Hilbers, C. W., and Nilges, M. (1998) *Proteins 31*, 370−382.
56. Massova, I., Martin, P., de Mel, S., Tanaka, Y., Edwards, B., and Mobashery, S. (1996) *J. Am. Chem. Soc. 118*, 12479−12480.
57. van Aalten, D. M. F., Bywater, R., Findlay, J. B. C., Hendlich, M., Hooft, R. W. W., and Vriend, G. (1996) *JCAMD 10*, 255−262.
58. van Gunsteren, W. F., and Berendsen, H. J. C. (1987) in *BIOMOS*, *Biomolecular Software*, Laboratory of Physical Chemistry, University of Groningen, The Netherlands.
59. Larsen, K. S., Zhang, K., and Auld, D. S. (1996) *J. Inorg. Chem. 64*, 149−162.
60. Argos, P., Garavito, R. M., Eventoff, W., and Rossman, M. G. (1978) *J. Mol. Biol. 126*, 141−158.
61. Matthews, B. W. (1988) *Acc. Chem. Res. 21*, 333−340.
62. Cha, J., and Auld, D. S. (1997) *Biochemistry 36*, 16019−16024.
63. Kraulis, P. J. (1991) *J. Appl. Crystallogr. 24*, 946−950.
64. Esnouf, R. M. (1997) *J. Mol. Graphics 15*, 132−134.
65. Bacon, D., and Anderson, W. F. (1988) *J. Mol. Graph. 6*, 219−220.
66. Merritt, E. A., and Murphy, M. E. P. (1994) *Acta Crystallogr. D50*, 869−873.
67. Nicholls, A., Sharp, K., and Honig, B. (1991) *Proteins 11*, 281−296.

BI000952H